JOC Article

Self-Aggregation of Synthetic Zinc Oxo-Bacteriochlorins Bearing Substituents Characteristic of Chlorosomal Chlorophylls

Michio Kunieda and Hitoshi Tamiaki*

Department of Bioscience and Biotechnology, Faculty of Science and Engineering, Ritsumeikan University, Kusatsu, Shiga 525-8577, Japan

tamiaki@se.ritsumei.ac.jp

Received October 4, 2004

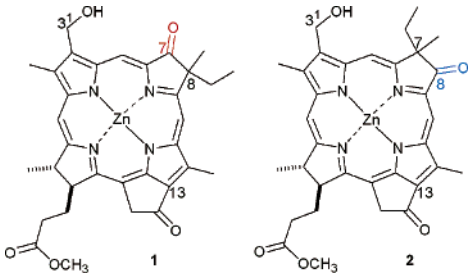

We prepared novel zinc 8-ethyl-8-methyl-7-oxo- and 7-ethyl-7-methyl-8-oxo-bacteriochlorins **1** and **2** possessing substituents characteristic of chlorosomal chlorophylls, exclusively observed in extramembraneous light-harvesting antennas of photosynthetic green bacteria. The electronic absorption spectra of monomeric **1** and **2** in THF were obviously different: the Q_y maximum of the former was 724 and that of the latter was 683 nm. This observed spectral difference was clearly explained by theoretical ZINDO/S calculation of their energetically minimized molecules. The optical properties of monomeric **1/2** were controlled by the electronic effect of the 7/8-oxo groups. Specific spectral changes in the electronic, CD, and FT-IR absorption spectra by dilution of the monomeric THF solutions of **1/2** with a 100/200-fold volume of cyclohexane showed the formation of chlorosomal self-aggregation species constructed by 13-C=O···H−O(3^1)···Zn and $\pi-\pi$ stacking. Especially, the red-shift values in the Q_y band of **1/2** by self-aggregation were 2450/1970 cm^{-1}, indicating that exciton interaction among the composite molecules in the self-aggregation of **1** was stronger than in those of **2**. Molecular model calculations for dodecamers of **1/2** based on a parallel chain arrangement gave partially different supramolecular structures; the specific hydrogen-bonding distances in **2**-dodecamer were larger than those of **1**-dodecamer, while both coordinations gave the same Zn−O distance. These modeling results showed that **1** was more tightly packed in the self-aggregates to give a larger red-shift value in the Q_y band by self-aggregation than **2**. The difference in the supramolecular structures is mainly ascribable to the steric effect of 8/7-dialkyl groups in self-aggregates of **1/2**.

Introduction

Natural photosynthesis primarily begins with efficient light-harvest of sunlight at antenna systems, which is followed by energy-migration and successive charge-separation stages. While the light-harvesting antenna systems of most photosynthetic organisms are complexes of pigments with oligopeptides based on their specific interactions, the major antenna of photosynthetic green bacteria (chlorosome) is constructed by self-aggregation of chlorophyllous pigments with no help from peptides.[1]

The intramolecular interactions of chlorosomal chlorophyll(Chl)s, bacteriochlorophyll(BChl)s-*c*/*d*/*e* are derived from their unique molecular structures (see Figure 1).[2] BChls-*c*/*d*/*e* have 3^1-hydroxy and 13-keto-carbonyl groups and a central magnesium atom along their Q_y axes (a line on N21 and N23 in Figure 1), and can self-aggregate

* Address correspondence to this author. Phone: (+81)77-566-1111. Fax: (+81)77-561-2659.

(1) (a) Olson, J. M. *Photochem. Photobiol.* **1998**, *67*, 61−75. (b) Blankenship, R. E.; Matsuura, K. In *Light Harvesting Antennas in Photosynthesis*; Green, B. R., Parson, W. W., Eds.; Kluwer Academic Publishers: Dordrecht, The Netherlands, 2003; pp 195−217. (c) Tamiaki, H. *Coord. Chem. Rev.* **1996**, *148*, 183−197.

(2) Scheer, H. In *Light Harvesting Antennas in Photosynthesis*; Green, B. R., Parson, W. W., Eds.; Kluwer Academic Publishers: Dordrecht, The Netherlands, 2003; pp 29−81.

10.1021/jo048263p CCC: $30.25
Published on Web 12/31/2004

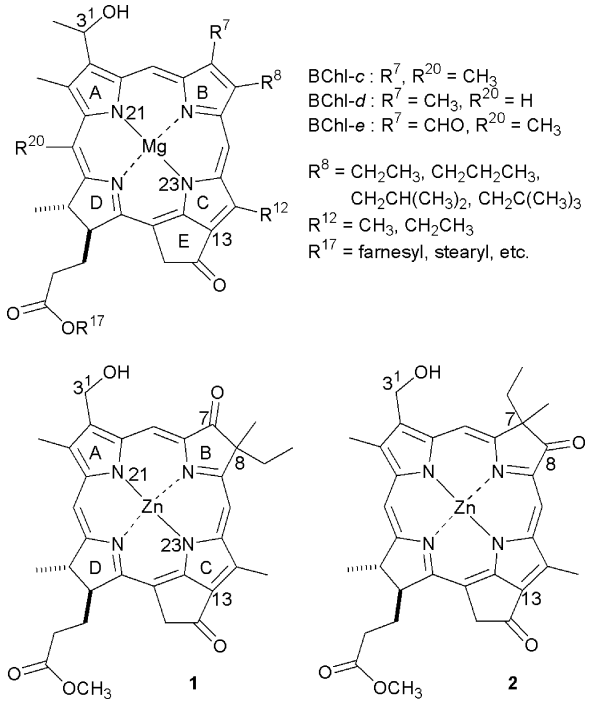

FIGURE 1. Molecular structures of BChls-*c*/*d*/*e* and synthetic zinc 7/8-oxo-bacteriochlorins **1**/**2** possessing chlorosomal substituents.

by specific bondings of their substituents as described below.[1,3] A 3^1-hydroxy group of one molecule coordinates to a central magnesium atom of the neighboring molecule and simultaneously hydrogen bonds to a 13-keto-carbonyl group of another molecule, constructing large three-dimensional self-aggregates. Such a chlorosomal self-aggregation is reproduced in vitro by using isolated natural BChls-*c*/*d*/*e*[1,4] and synthetic stable models possessing the above three characteristic substituents.[5] Their chlorosomal self-aggregates are spontaneously formed when their monomeric solution (typically methanol or THF as a solvent) is diluted with a large amount of nonpolar organic solvents or water. The self-aggregates of synthetic models were highly stable compared with the natural antenna systems, and suitable for construction of artificial light-harvesting antennas,[6] but their optical properties were limited due to their current skeletal π-conjugate systems. Natural BChls-*c*/*d*/*e* and almost all their synthetic models have a chlorin π-conjugate (one reduced pyrrole at ring D in Figure 1) whose monomeric Q_y absorption peaks are situated in the region of about 620−660 nm, and their self-aggregation causes the Q_y absorption maxima to shift around 670−760 nm.[5] A variety of optical properties of chlorosomal self-aggregates are of great advantage for their utilization as photoactive nanodevices.

Recently, we reported chlorosomal self-aggregation of 3-(1-hydroxyethyl)bacteriopyrochlorophyll-*a* possessing a bacteriochlorin π-conjugate (two reduced pyrroles at rings B and D in Figure 1), which absorbed lights in the near-infrared region.[7] Electronic absorption properties of the self-aggregates including the Q_y maximum of 860 nm were significantly different from those of the systems based on chlorin π-conjugates. The reported self-aggregative bacteriochlorin had two hydrogen atoms at the 7,8-positions and was readily oxidized to the corresponding chlorin π-conjugate, so that stable molecules were required for self-aggregative bacteriochlorins as a chlorosome model. Thus we focused our attention on oxo-bacteriochlorin molecules previously reported by Pandey et al.[8] Such molecules are chemically stable because they have no hydrogen atom at the 7- and 8-positions, and cannot give undesired dehydrogenated chlorin pigments. We designed self-aggregative zinc oxo-bacteriochlorins **1** and **2** bearing the chlorosomal substituents as drawn in Figure 1. In addition to the dialkylation of the 8- or 7-position, substitution of magnesium with zinc atom as the central metal[5a] enlarged the chemical stability on these chromophores. Here we report on syntheses of stable **1** and **2** by modifying easily available Chl-*a*, and their self-aggregation in nonpolar organic solvents.

Results and Discussion

Synthesis of Self-Aggregative Zinc Oxo-Bacteriochlorins 1 and 2. As shown in Scheme 1, zinc 7/8-oxo-bacteriochlorins **1**/**2** were available from methyl 3-formyl-7,8-*cis*-dihydroxy-pyropheophorbide-*a* (**3**),[8] which was easily prepared from naturally occurring Chl-*a*. Pinacol−pinacolone rearrangement of **3** in concentrated sulfuric acid afforded the corresponding 7-oxo- and 8-oxo-bacteriochlorins **4** and **5** as a mixture. In the previous

(3) Holzwarth, A. R.; Schaffner, K. *Photosynth. Res.* **1994**, *41*, 225−233.

(4) (a) Bystrova, M. I.; Mal'tgocheva, I. N.; Krasnovskii, A. A. *Mol. Biol.* **1979**, *13*, 440−451. (b) Smith, K. M.; Kehres, L. A.; Fajer, J. *J. Am. Chem. Soc.* **1983**, *105*, 1387−1389. (c) Brune, D. C.; Nozawa, T.; Blankenship, R. E. *Biochemistry* **1987**, *26*, 8644−8652. (d) Balaban, T. S.; Leitich, J.; Holzwarth, A. R.; Schaffner, K. *J. Phys. Chem. B* **2000**, *104*, 1362−1372. (e) Ishii, T.; Kimura, M.; Yamamoto, T.; Kirihata, M.; Uehara, K. *Photochem. Photobiol.* **2000**, *71*, 567−573. (f) Mizoguchi, T.; Hara, K.; Nagae, H.; Koyama, Y. *Photochem. Photobiol.* **2000**, *71*, 596−609. (g) Steensgaad, D. B.; Wacherbarth, H.; Hildebrandt, P.; Holzwarth, A. R. *J. Phys. Chem. B* **2000**, *104*, 10379−10386. (h) Saga, Y.; Matsuura, K.; Tamiaki, H. *Photochem. Photobiol.* **2001**, *74*, 72−80. (i) Mizoguchi, T.; Saga, Y.; Tamiaki, H. *Photochem. Photobiol. Sci.* **2002**, *1*, 780−787. (j) Umetsu, M.; Hollander, J. G.; Matysik, J.; Wang, Z.-Y.; Adschiri, T.; Nozawa, T.; de Groot, H. J. M. *J. Phys. Chem. B* **2004**, *108*, 2726−2734.

(5) (a) Tamiaki, H.; Amakawa, M.; Shimono, Y.; Tanikaga, R.; Holzwarth, A. R.; Schaffner, K. *Photochem. Photobiol.* **1996**, *63*, 92−99. (b) Balaban, T. S.; Tamiaki, H.; Holzwarth, A. R.; Schaffner, K. *J. Phys. Chem. B* **1997**, *101*, 3424−3431. (c) Kureishi, Y.; Tamiaki, H. *J. Porphyrins Phthalocyanines* **1998**, *2*, 159−169. (d) Yagai, S.; Miyatake, T.; Tamiaki, H. *J. Photochem. Photobiol. B* **1999**, *52*, 74−85. (e) Tamiaki, H.; Kubo, M.; Oba, T. *Tetrahedron* **2000**, *56*, 6245−6257. (f) Yagai, S.; Miyatake, T.; Shimono, Y.; Tamiaki, H. *Photochem. Photobiol.* **2001**, *73*, 153−163. (g) Yagai, S.; Miyatake, T.; Tamiaki, H. *J. Org. Chem.* **2002**, *67*, 49−58. (h) Tamiaki, H.; Amakawa, M.; Holzwarth, A. R.; Schaffner, K. *Photosynth. Res.* **2002**, *71*, 59−67. (i) Tamiaki, H.; Kimura, S.; Kimura, T. *Tetrahedron* **2003**, *59*, 7423−7435. (j) Tamiaki, H.; Omoda, M.; Saga, Y.; Morishita, H. *Tetrahedron* **2003**, *59*, 4337−4350. (k) Sasaki, S.; Omoda, M.; Tamiaki, H. *J. Photochem. Photobiol. A* **2004**, *162*, 307−315. (l) Miyatake, T.; Tamiaki, H.; Fujiwara, M.; Matsushita, T. *Bioorg. Med. Chem.* **2004**, *12*, 2173−2178. (m) Sasaki, S.; Tamiaki, H. *Bull. Chem. Soc. Jpn.* **2004**, *77*, 797−800.

(6) (a) Tamiaki, H.; Miyatake, T.; Tanikaga, R.; Holzwarth, A. R.; Schaffner, K. *Angew. Chem., Int. Ed. Engl.* **1996**, *35*, 772−774. (b) Miyatake, T.; Tamiaki, H.; Holzwarth, A. R.; Schaffner, K. *Helv. Chim. Acta* **1999**, *82*, 797−810. (c) Prokhorenko, V. I.; Holzwarth, A. R.; Müller, M. G.; Schaffner, K.; Miyatake, T.; Tamiaki, H. *J. Phys. Chem. B* **2002**, *106*, 5761−5768. (d) Saga, Y.; Akai, S.; Miyatake, T.; Tamiaki, H. *Chem. Lett.* **2004**, *33*, 544−545.

(7) Kunieda, M.; Mizoguchi, T.; Tamiaki, H. *Photochem. Photobiol.* **2004**, *79*, 55−61.

(8) Pandey, R. K.; Isaac, M.; MacDonald, I.; Medforth, C. J.; Senge, M. O.; Dougherty, T. J.; Smith, K. M. *J. Org. Chem.* **1997**, *62*, 1463−1472.

SCHEME 1. Synthesis of Self-Aggregative Zinc Oxo-bacteriochlorins 1 and 2[a]

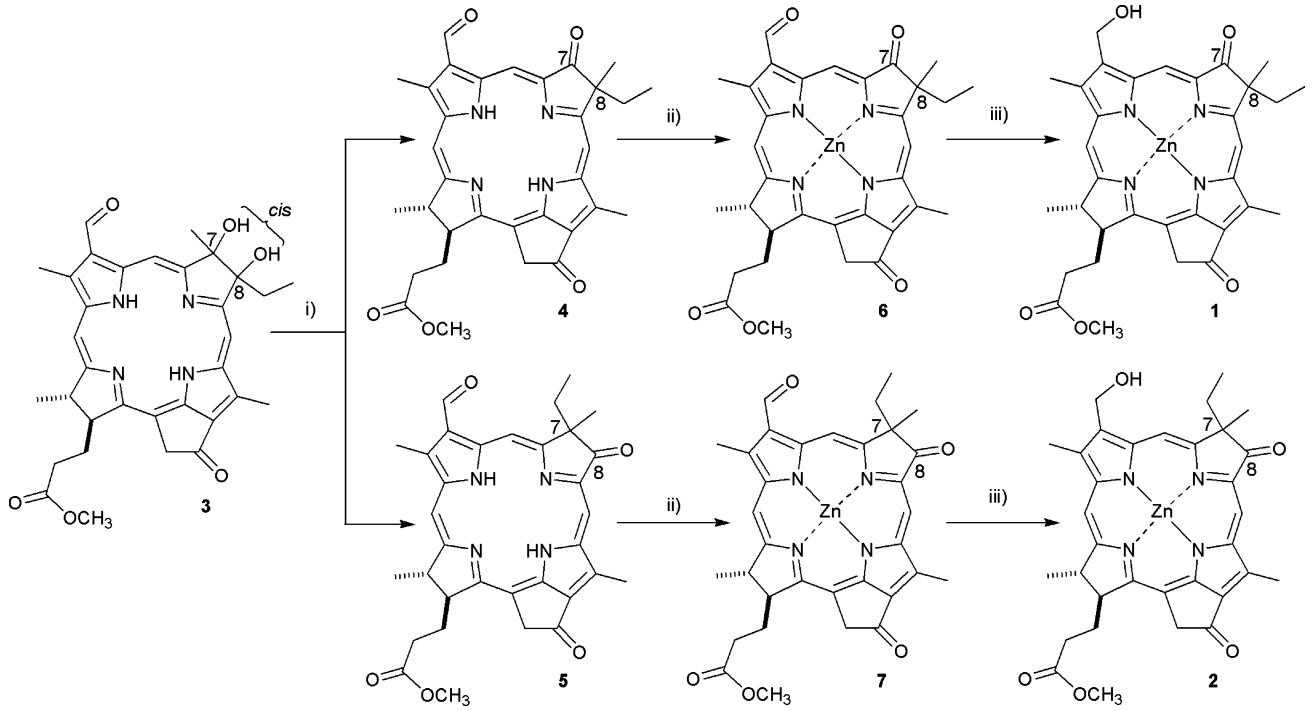

[a] Reagents and conditions: (i) concentrated H_2SO_4, 7,8-regioisomeric separation with deactivated aluminum oxide column; (ii) $Zn(OAc)_2 \cdot 2H_2O$/methanol, $CHCl_3$, reflux; (iii) tBuNH$_2 \cdot BH_3$, CH_2Cl_2.

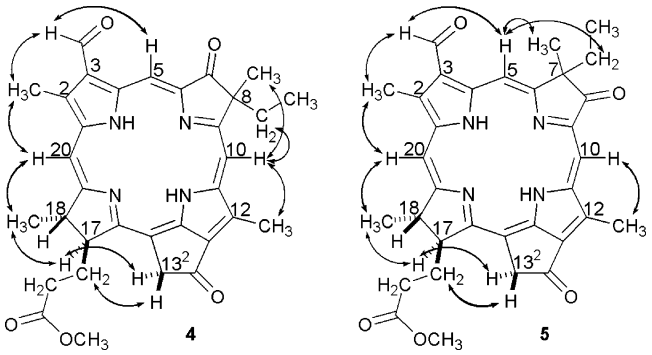

FIGURE 2. Observed NOE correlations of 7/8-oxo-bacteriochlorins **4** and **5**.

report,[8] no 7,8-regioisomeric separation had been achieved but the isomers were separated on a deactivated aluminum oxide column (6 w/w % water/aluminum oxide) with dichloromethane as an eluent to give the fast-moving orange followed by slow-moving brown fractions. Molecular structures of the separated regioisomers were completely determined by their ^{1}H−^{1}H COSY/NOESY and FAB-MS: observed NOE correlations of first-moving (left) and slow-moving compounds (right) as shown in Figure 2. First, we assigned 17-H of each of **4** and **5** by NOE correlation with specific germinal coupled 13^1-CH, then 18-CH$_3$, 20-H, 2-CH$_3$, 3-CHO, and 5-H by NOE correlations in the clockwise direction of the molecule, and finally the remaining *meso*-proton at around 9 ppm as 10-H. While the first elution showed obvious NOE correlations between 10-H and the dialkyl group (CH$_3$ and CH$_2$CH$_3$) and no correlation between 5-H and the dialkyl group, the second showed reversed NOE correlations, indicating that the first and second were 3-formyl-7-oxo- and 8-oxo-bacteriochlorins **4** and **5**, respectively. Isolated yields of **4** and **5** were 42% and 21%, showing that the 7-methyl migration in the rearrangement of **3** was more favorable than the 8-ethyl migration. Similar tendencies were observed in the pinacol−pinacolone rearrangements of 3-acetyl- and 3-ethyl-7,8-*cis*-diols **8** and **9** (Scheme 2): formation of 3-acetyl- and 3-ethyl-7/8-oxo-bacteriochlorins **10/11** (41%/20%) and **12/13** (53%/18%).

A chloroform solution of 3-formyl-7-oxo- or 8-oxo-bacteriochlorins **4** or **5** was refluxed with a saturated methanol solution of zinc acetate[5a] to afford the corresponding zinc complex **6** or **7** (85%/83%), respectively. Selective reduction of the 3-formyl group[5a] gave the desired self-aggregative zinc 3-hydroxymethyl-7-oxo- and 8-oxo-bacteriochlorins **1** and **2** (92%/85%). All the synthetic molecules were identified by their NMR and FAB-MS spectra.

Optical Properties of Monomeric 1 and 2 in THF. In THF, **1** and **2** were monomeric (solid lines of Figure 3A,C) because their electronic absorption bands were sharp and the CD bands (solid lines of Figure 3B,D) were small. The $Q_y(0,0)$ bands of **1** and **2** were situated at 724 and 683 nm with the full width at half-maximum (fwhm) of 270 and 570 cm^{-1}, respectively. These bands were accompanied by the corresponding vibrational bands at the shorter wavelength region. Regioisomers **1** and **2** had relatively small $Q_x(0,0)$ bands at 580 and 565 nm, respectively, with the corresponding vibrational components at the shorter wavelength. Their Soret bands were situated in the region up to 460 nm with various components. An obvious difference between the electronic absorption spectra of **1** and **2** is especially found in the $Q_y(0,0)$ peak, which is important in determining the emission properties of chlorophyllous pigments.

SCHEME 2. Pinacol−Pinacolone Rearrangement of 3-Acetyl- and 3-Ethyl-7,8-*cis*-diols 8 and 9 by Concentrated H_2SO_4

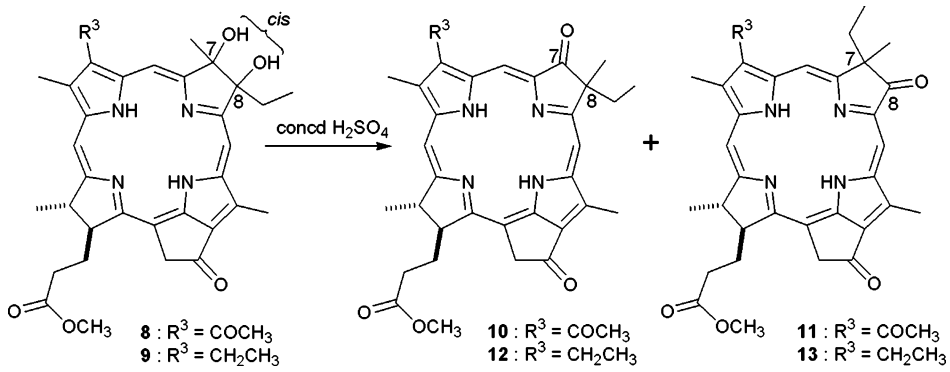

TABLE 1. Absorption Maxima (nm) Observed for 1 and 2 in THF (exptl) and Estimated by ZINDO/S Calculation (calcd)

	$Q_y(0,0)$		$Q_x(0,0)$	
compd	exptl	calcd	exptl	calcd
1	724	727	580	566
2	683	698	565	556

The difference in Q_y/Q_x peaks between **1** and **2** was clearly reproduced by ZINDO/S calculations of their energetically minimized molecules.[5e,9] A central zinc atom of **1** and **2** was coordinated with a THF molecule from the other side of the 17-propionate side chain, and energetically minimized by MM+/PM3 calculation. The resulting molecule was run on ZINDO/S calculation to give estimated electronic absorption maxima of **1** and **2** as summarized in Table 1. The calculations afforded estimated Q_y maximum of **1** at 727 nm (exptl 724 nm), which was more red-shifted than that of **2** at 698 nm (exptl 683 nm). The estimated $Q_x(0,0)$ maximum of **1** at 566 nm (exptl 580 nm) was also more red-shifted than that of **2** at 556 nm (exptl 565 nm). The electron-withdrawing 7- and 8-oxo groups in **1** and **2** played definitive roles in their monomeric optical properties, similarly to 7/8-formyl chlorophyll derivatives reported by our group.[5m] The monomeric optical properties of **1/2** were thus controlled by the situations of 7- and 8-oxo groups, i.e., their electronic effect.

Self-Aggregation of Zinc Oxo-Bacteriochlorins 1 and 2 in THF/Cyclohexane. When a monomeric THF solution of **1** or **2** was diluted with a 100- or 200-fold volume of cyclohexane, their self-aggregation was observed from electronic absorption (broken lines in Figure 3A,C) and CD spectral analyses (broken lines in Figure 3B,D) as described below. Here **1** and **2** were used as 8- and 7-epimeric mixtures.[10]

In 1 v/v % THF/cyclohexane, **1** showed a red-shifted and broadened Q_y band at 880 nm with 720 cm^{-1} of the fwhm (broken line of Figure 3A), while the monomeric Q_y band was situated at 724 nm (fwhm = 270 cm^{-1}). The CD spectrum of **1** in the nonpolar organic solvent (broken line of Figure 3B) showed intense signals at around the Q_y and Soret regions. Since similar spectral changes were observed in self-aggregation of natural[4] and synthetic chlorosomal (bacterio)chlorins,[5,7] **1** self-aggregated in the nonpolar organic solvent to form large oligomers. A red-shift value in the Q_y band by self-aggregation of **1** was 2450 cm^{-1} (724→880 nm), which was larger than typical values of natural BChls-*c*/*d*/*e* (1200−1700 cm^{-1}) possessing the 3-(1-hydroxyethyl) group and synthetic chlorosomal chlorins (ca. 2000 cm^{-1}) possessing the 3-hydroxymethyl group. Self-aggregation of chlorosomal zinc chlorins possessing the 3-hydroxymethyl group showed more red-shifted Q_y bands than the 3-(1-hydroxyethyl) type due to a less steric hindrance around the interactive 3^1-hydroxy group.[5f] Since the bacteriochlorin possessing the 3-(1-hydroxyethyl) group gave a red-shift value of 2170 cm^{-1} in the Q_y band by self-aggregation,[7] a red-shift value of 2450 cm^{-1} is acceptable for the self-aggregation of the present bacteriochlorin **1** possessing the 3-hydroxymethyl group.

Similar self-aggregation of **2** occurred in 0.5 v/v % THF/cyclohexane to give a red-shifted Q_y band at 789 nm (broken line in Figure 3C), compared with the monomeric Q_y band at 683 nm. Intense CD signals were observed around the newly appearing electronic absorption peaks (broken line in Figure 3D). Therefore, 8-oxo-**2** self-aggregated in the nonpolar organic solvent to form chlorosomal self-aggregates. The red-shift value in the Q_y band by self-aggregation of **2** was 1970 cm^{-1} (683→789 nm), which was less than that of **1**, and self-aggregates of **2** could not be formed in 1 v/v % THF/cyclohexane, indicating that self-aggregates of **2** were formed by relatively weak interactions among the molecules, compared with those of **1**. The different red-shift values in the Q_y band by self-aggregation of **1** and **2** are discussed below.

FT-IR Spectra of Self-Aggregates of 1 and 2. Among specific interactions used in chlorosomal self-aggregation, hydrogen bonding between 3^1-hydroxy and 13-keto-carbonyl groups is easily observed on FT-IR

(9) (a) Linnanto, J.; Korppi-Tommola, J. *J. Phys. Chem. A* **2001**, *105*, 3855−3866. (b) Tamiaki, H.; Watanabe, T.; Kunieda, M. *Res. Chem. Intermed.* **2005**, *31*, in press.

(10) The 8- or 7-epimeric separation of 3-formyl-7-oxo-**6** or 8-oxo-**7** was easily done by normal-phase HPLC (see Figure S1 in the Supporting Information), and reduction of the resulting 8- or 7-epimerically pure sample gave the corresponding 8-epimerically pure **1**-f1 and **1**-f2, or 7-epimerically pure **2**-f1 and **2**-f2: f1 and f2 mean the first and second elutions on the HPLC separation. The self-aggregations of separated **1**-f1 and **1**-f2 had almost the same spectra except for time-dependent CD signals: the CD spectra were different just after preparation of the solution but became the same after standing for 1 day (see Figure S2A,B). Similar results were obtained for **2**-f1 and **2**-f2 (see Figure S2C,D). In this paper we focused on the difference between 7-oxo-**1** and 8-oxo-**2**, and used their epimeric mixtures to compare the optical properties of the regioisomers.

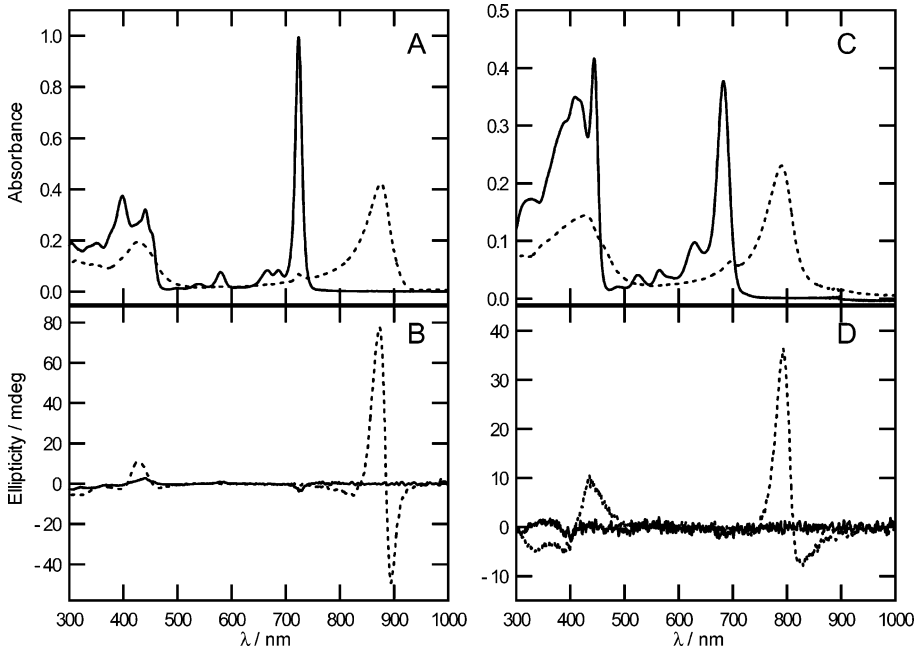

FIGURE 3. Electronic (upper) and CD absorption spectra (bottom) of zinc 7-oxo-bacteriochlorin **1** (left, A and B) in THF (solid) and 1 v/v % THF/cyclohexane (broken), and of zinc 8-oxo-bacteriochlorin **2** (right, C and D) in THF (solid) and 0.5 v/v % THF/cyclohexane (broken).

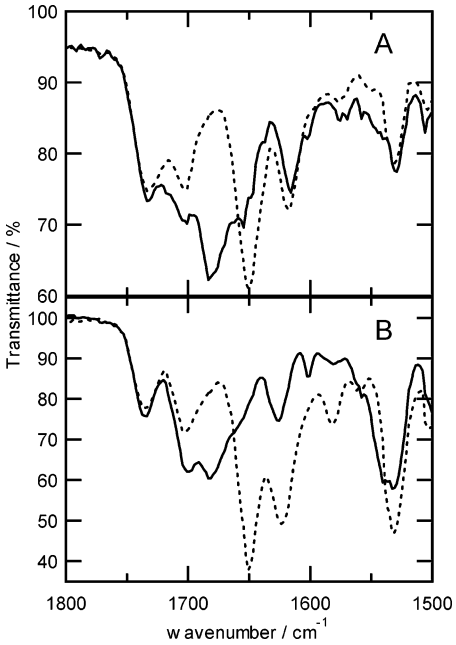

FIGURE 4. FT-IR spectra of thin film aggregates of **1** (A) and **2** (B) with (solid) or without pyridine vapor (broken).

spectra as shown in the downshifted 13-keto-carbonyl vibrational signal.[4g,5a,b,d,h,11] Reminded that the two keto-carbonyl groups on the rings B and E in **1** and **2** potentially form hydrogen bonds with a 3^1-hydroxy group of the neighboring molecule in the self-aggregates, FT-IR spectra of monomers and oligomers of **1/2** were analyzed. They were measured in the solid states, since the self-aggregates of neither **1** nor **2** could be sufficiently dissolved in nonpolar organic solvents. Figure 4 shows FT-IR spectra of **1** (A) and **2** (B) in a solid thin film with or without pyridine vapor. Oxo-bacteriochlorins **1** and **2** were dissolved in THF/cyclohexane and the resulting solutions were dropped onto an aluminum-coated plate and dried to give their thin film aggregates. Electronic and CD absorption spectra of the thin film of **1** (Figure S3A,B in the Supporting Information) were similar to those in a nonpolar organic solvent (broken lines in Figure 3A,C), indicating **1** self-aggregated in the solid state similarly as in the solution. Similar results were obtained in the film aggregates of **2** (Figure S3C,D).

FT-IR spectrum of the prepared film aggregates of **1** (broken line in Figure 4A) showed four peaks in the region from 1600 to 1750 cm^{-1}, of which 1616- and 1734-cm^{-1} peaks were assigned as vibrational bands to the π-skeletal and 17^2-C=O moieties, respectively, compared with the reported data.[5a] The remaining two peaks were situated at 1703 and 1651 cm^{-1} which were ascribable to keto-carbonyl groups on the $7/13^1$-positions. Treatment of the film by pyridine vapor induced de-aggregation as indicated by a gradual appearance of the 1682-cm^{-1} peak and a concomitant decrease of the 1651-cm^{-1} peak, and finally (>1 h) an IR spectrum (solid line of Figure 4A) was obtained. Intensities of these two peaks equilibrated with pyridine vapor were gradually changed in air to afford the initial spectrum of the film aggregates (see Figure S4). Throughout the de-aggregation and re-aggregation processes, the 1703-cm^{-1} peak did not show any shift. Generally the 13-C=O signal of monomeric zinc chlorin is found at around 1690 cm^{-1}, and that of self-aggregated zinc chlorin is downshifted by ca. 30−40 cm^{-1} to give a 13-keto-carbonyl signal at around 1660−1650 cm^{-1},[5a,h] then the signals at 1651 and 1682 cm^{-1} would be due to oligomeric and monomeric 13-C=O vibrational stretchings, respectively. This assignment is supported by the fact that sterically less hindered 13-C=O is more accessible to any other functional groups than C7=O possessing two neighboring alkyl groups. The 1682-cm^{-1} peak of **1** was also consistent with the 1681-cm^{-1} peak in zinc complex **14** of 3-ethyl-7-oxo-bacteriochlorin **12**

lacking the 3^1-hydroxy group in THF (Figure S5A), confirming that the 1682-cm^{-1} peak was assigned to the monomeric 13-C=O band of **1**. The 1703-cm^{-1} peak would thus be a vibrational signal of the 7-oxo group free from any interaction, which was supported by the presence of the 1701-cm^{-1} peak of monomeric **14** in THF. The unchanged 1703-cm^{-1} peak through the de- and re-aggregation processes indicated that the more sterically hindered 7-oxo group was not included in the chlorosomal self-aggregation of **1** as 7-CHO in natural BChl-*e*[4g] and synthetic BChl-*f* derivatives.[5m] It was noteworthy that the de-aggregation of oligomeric **1** by pyridine vapor had not been achieved completely and the re-aggregation occurred by evaporation of pyridine, showing that the self-aggregates of **1** were strongly constructed by the hydrogen-bonding networks.

Similar vibrational measurements were carried out with 8-oxo-**2** (Figure 4B). The FT-IR spectrum of the thin film before pyridine treatment (broken line of Figure 4B) also showed four peaks in the region from 1600 to 1750 cm^{-1}. Besides skeletal and 17^2-C=O bands at 1623 and 1734 cm^{-1}, assignments of the remaining two peaks were done in a similar manner as in **1**. Treatment of pyridine vapor immediately caused the appearance of a new peak at 1683 cm^{-1} with almost complete disappearance of the 1651-cm^{-1} peak (solid line of Figure 4B), indicating the self-aggregates changed to monomers: 1651 cm^{-1} for 13-C=O in self-aggregates and 1683 cm^{-1} in its monomer. The 1683-cm^{-1} peak of **2** after treatment of pyridine vapor was also consistent with the 1681-cm^{-1} peak of zinc complex **15** of 3-ethyl-8-oxo-bacteriochlorin **13** in THF (Figure S5B), and the remaining 1702-cm^{-1} peak was thus a vibrational signal of the 8-oxo group free from any interaction, which was supported by the presence of the 1700-cm^{-1} peak of **15** in THF. The peak at 1702 cm^{-1} for the 8-oxo group was not changed during the de-aggregation and the 8-oxo group of **2** was not included in the hydrogen-bonding network of self-aggregates or in the 7-oxo group of **1**. No further change in the FT-IR spectra of monomeric **2** was observed even after standing in air for a long time, indicating that the hydrogen bonding in the self-aggregation of **2** is weaker than that of **1**.

Molecular Model Calculations for Dodecamers of 1 and 2. From the above electronic, CD, and FT-IR absorption spectral analyses, **1** and **2** self-aggregated to form chlorosomal self-aggregates by specific interactions among the 3^1-hydroxy, 13-keto-carbonyl groups, and central zinc atom, and did not use any 7- and 8-oxo groups for the formation of their chlorosomal self-assemblies. While based on the same construction motif, self-aggregates of **1** and **2** gave different red-shift values in the Q_y bands, indicating that their supramolecular structures were slightly modified from each other. These differences were estimated by the following molecular model calculation. As the chlorosomal self-aggregates, a parallel chain model[1c,3,5a,f] was employed in the present calculation, because almost all natural and artificial systems had been clearly characterized by this model. Scheme 3 shows a schematic drawing of parallel chain dodecamer of **1/2**. Coordination bonding between the 3^1-hydroxy group of one molecule and the zinc atom of another, constructing a linear "column" (boxed in Scheme 3), connects with the neighboring column by hydrogen bonding between the 3^1-hydroxy group of one column and

SCHEME 3. Schematic Representation of Dodecamer of 1/2 Based on a Parallel Chain Model

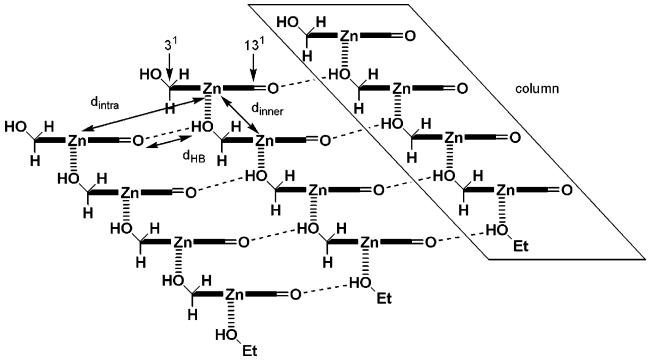

TABLE 2. Estimated Atomic Distances (Å) of Neighboring Zn-to-Zn in a Column (d_{inner}), Zn-to-Zn between Neighboring Columns (d_{intra}), and H-to-O in the Hydrogen Bond of 3^1-OH with 13-C=O (d_{HB})[a]

	d_{inner}	d_{intra}	d_{HB}
1′-dodecamer	6.60	9.22	2.07
2′-dodecamer	6.60	9.60	2.35
1″-dodecamer	6.54	9.21	2.09
2″-dodecamer	6.53	9.24	2.10

[a] All the values listed are averages of distances from energetically minimized dodecamers.

the 13-keto-carbonyl groups of another to make a large aggregate. In the present calculation, we used 8,8-dimethyl-7-oxo-**1′** and 7,7-dimethyl-8-oxo-**2′** as alternatives of **1** and **2** (8/7-ethyl → 8/7-methyl group) to avoid consideration of the stereochemistry at the 8- and 7-positions.

Table 2 shows the averaged values of estimated atomic distances of neighboring Zn-to-Zn in a column (d_{inner}), Zn-to-Zn between neighboring columns (d_{intra}), and H-to-O in the hydrogen bond of 3^1-OH with 13-C=O (d_{HB}) in energetically minimized dodecamers of **1′** and **2′**. Inner-column distances d_{inner} in **1′**- and **2′**-dodecamers take the same values of 6.60 Å, indicating that both their $\pi-\pi$ interaction and coordination in a column were unchanged. On the contrary, their intracolumn distances d_{intra} were different: 9.22 Å for **1′**-dodecamer and 9.60 Å for **2′**-dodecamer. The large intracolumn distance of **2′**-dodecamer should decrease the $\pi-\pi$ stacking among the columns, and would be limited from growing into a large oligomer. Such weak interactions among the composite molecules in **2′**-dodecamer should suppress the red-shift of the Q_y band, compared with **1′**-dodecamer. This explanation would hold in the observed different red-shifts of self-aggregates of **1** and **2**; similar weak intracolumn interactions in self-aggregates of **2** resulted in a less red-shifted Q_y band (1970 cm^{-1}), compared with 2450 cm^{-1} in self-aggregated **1**.

The above decrease in $\pi-\pi$ stacking among columns in the **2′**-dodecamer causes an increase in d_{HB} (2.07→2.35 Å), and vice versa. Such a theoretical explanation is consistent with the observed FT-IR shifts of the 13-keto-carbonyl stretching bands in solid films of **1/2**-self-aggregates: by treatment of pyridine vapor, $\nu_{13\text{-C=O}}$ of $(\mathbf{2})_n$ largely disappeared and that of $(\mathbf{1})_n$ partially; after exposure to air that of monomeric **2** remained but that of **1** changed to that of $(\mathbf{1})_n$. One of the driving forces in

self-aggregation, hydrogen bonding of 3^1-OH with 13-C=O, was different in the self-aggregates of **1**/**2**, which was clearly confirmed by the experimental and theoretical results described above.

To clarify the factor of differences in supramolecular structures of self-aggregated **1** and **2**, we calculated two additional dodecamers of **1**″ and **2**″ which had dihydrogen atoms at the 8- and 7-positions replaced from the 8- and 7-dialkyl groups of original **1** and **2**. The calculated results afforded the three averaged distances in **1**″- and **2**″-dodecamers as summarized in Table 2: energetically minimized **1**″- and **2**″-dodecamers lacking 8- and 7-dialkyl groups showed 6.54 and 6.53 Å for d_{inner}, 9.21 and 9.24 Å for d_{intra}, and 2.09 and 2.10 Å for d_{HB}, respectively. By substituting the 7-dimethyl groups of **2**′-dodecamer with two hydrogens, steric hindrance around the B-rings decreased and resulted in similar d_{intra} and d_{HB} values with those of **1**″-dodecamer. Such a substitution in **1**′→**1**″ gave limited changes of estimated atomic distances in **1**′/**1**″-dodecamers. Therefore, the 7-dialkyl groups of **2** actually caused a disturbance in the molecular stacking, while the 8-dialkyl groups of **1** did not sterically disturb the formation of self-aggregates.[12] The optical properties of oligomeric **1**/**2** were controlled by the situations of the 8/7-dialkyl groups, i.e., their steric effect.

Conclusion

We succeeded to 7,8-regioisomerically separate oxobacteriochlorins **4** and **5** prepared by pinacol−pinacolone rearrangement of 7,8-*cis*-diol **3**. The regioisomerically pure **4** and **5** were modified into zinc 3-hydroxymethylated 8-ethyl-8-methyl-7-oxo- and 7-ethyl-7-methyl-8-oxo-bacteriochlorins **1** and **2**. In THF/cyclohexane, both **1** and **2** self-aggregated in a similar manner with natural and artificial chlorosomal pigments: Zn···O(3^1)−H···O=C(13) and $\pi-\pi$ interaction. The linear situation of 3^1-OH, Zn, and 13-C=O along the Q_y axis in a molecule played a significant role in the self-aggregation, while the more sterically hindered 7/8-oxo group in **1**/**2** was free in their self-aggregates. Optical properties of monomeric 7-oxo-**1** and 8-oxo-**2** were significantly different, being controlled by the situation of the electron-withdrawing oxo group at the 7- and 8-positions (electronic effect of the oxo-substituents). In contrast, supramolecular structures of **1** and **2** were controlled by the situation of 8- and 7-dialkyl groups (steric effect of the methyl/ethyl groups), leading to different red-shift values in the Q_y band by self-aggregation. Especially, the red-shift value of the Q_y band by self-aggregation of **1** was 2450 cm^{-1}, which was the largest value of chlorosomal self-aggregation of natural and synthetic chlorophyllous pigments.

Experimental Section

(a) Molecular Modeling: Monomeric Zinc Complexes 1 and 2. The central zinc atom of a molecule was coordinated with the THF molecule from the *anti*-direction to the 17-propionate. **1**·THF and **2**·THF were energetically minimized by MM+/PM3 calculation until the energy gradient reached less than 0.01.[5f] The resulting molecule was run on the ZINDO/S calculation with CI space of (10,10) for the HOMO/LUMO[9] to give an estimated electronic absorption maxima of oxo-bacteriochlorins.

Dodecamers of 1′ and 2′. Energetically minimized zinc 3-hydroxymethyl-8,8-dimethyl-7-oxo-**1**′ and 7,7-dimethyl-8-oxo-**2**′ with a coordinated ethanol molecule from the *anti*-direction of the 17-propionate side chain were obtained by the above calculation procedure (MM+/PM3). The coordinating ethanol molecule was removed, and then coordination-bondings between the zinc atom of one molecule and the 3^1-oxygen atom of another were performed from the *anti*-direction of the 17-propionate side chain to make a linear tetramer.[3,5f] The terminal zinc atom was ligated with ethanol, and then energetically minimized by MM+/PM3 calculation until the energy gradient reached less than 0.01. The atomic distances between 13^1-oxygen atoms of a tetramer and hydrogen atoms of the 3^1-hydroxy group of another tetramer were forced at 2.5 Å to construct a dodecamer. Energy minimization by MM+ with a force field constant of 1000 was carried out until the energy gradient reached less than 0.01. After the minimization, the restraint was removed and then again calculated until it reached a 0.01 energy gradient to give an energetically minimized dodecamer.

The atomic distances listed in Table 2 were measured in the resulting **1**′- and **2**′-dodecamers. The value of d_{inner} was averaged from $3 \times 3 = 9$ atomic distances between the central zinc atom of one molecule and that of the coordinated molecule in a column. The value of d_{intra} was averaged from $4 \times 2 = 8$ atomic distances between the central zinc atom of one molecule and that of the closed molecule in another column. The value of d_{HB} was averaged from $3 \times 2 = 6$ atomic distances between the hydrogen atom of the 3^1-hydroxy group and the oxygen atom of the hydrogen-bonded 13-keto-carbonyl group.

Dodecamers of 1″and 2″. The dimethyl groups at the 8- or 7-positions of the energetically minimized **1**′- or **2**′-dodecamers were replaced with two hydrogen atoms, and then the resulting dodecamers were calculated by MM+ under the restraints of hydrogen-bonding lengths. After removal of the restraints, energy minimization was done again to give energetically minimized **1**″- and **2**″-dodecamers.

(b) Synthesis: Noncommercial Compounds. Methyl 7,8-*cis*-dihydroxy-pyropheophorbide-*d* (**3**),[8] methyl 3-acetyl-3-devinyl-7,8-*cis*-dihydroxy-pyropheophorbide-*a* (**8**),[5d,k] and methyl 3-devinyl-3-ethyl-7,8-*cis*-dihydroxy-pyropheophorbide-*a* (**9**)[5d] were prepared according to the reported procedures.

Pinacol−Pinacolone Rearrangement.[8] 7,8-*cis*-Dihydroxybacteriochlorin (70 μmol) was dissolved in concentrated sulfuric acid (20 mL) and stirred for 30 min at room temperature under nitrogen. The reaction mixture was diluted with ice−water and extracted with chloroform until the aqueous phase became colorless. The organic layer was washed with water and dried over Na_2SO_4. After concentration, the residue was chromatographed on an alumina column deactivated with 6 w/w % water with dichloromethane as an eluent to afford 7-oxo- and 8-oxo-bacteriochlorins as the fast- and slow-moving elutions, respectively. Separated samples were recrystallized from dichloromethane/hexane to give pure regioisomers as a 1:1 epimeric mixture at the ethylated and methylated positions (the 8/7-position for 7/8-oxo-bacteriochlorin). *cis*-Diol → 7-oxo + 8-oxo: 3-formyl-**3** → **4** (42%) + **5** (21%), 3-acetyl-**8** → **10** (41%) + **11** (20%), and 3-ethyl-**9** → **12** (53%) + **13** (18%).

Methyl 7-demethyl-8-methyl-7-oxo-pyropheophorbide-*d* (4): Vis (CH_2Cl_2) λ_{max} 737 (rel intensity, 1.67), 696 (0.10), 665 (0.09), 554 (0.18), 523 (0.18), 436 (0.91), 421 (1.0), 399 nm (0.89); ^{1}H NMR ($CDCl_3$) δ 11.63 (1H, s, 3-CHO), 10.07/06 (1H, s, 5-H), 8.91 (1H, s, 10-H), 8.88 (1H, s, 20-H), 5.31, 5.17 (each 1H, d, J = 19 Hz, 13^1-CH_2), 4.52 (1H, m, 18-H), 4.34 (1H, m, 17-H), 3.75 (3H, s, 2-CH_3), 3.66 (3H, s, 12-CH_3), $3.64_1/63_6$ (3H,

(11) (a) Amakawa, M.; Tamiaki, H. *Bioorg. Med. Chem.* **1999**, *7*, 1141−1144. (b) Morishita, H.; Tamiaki, H. *Bioorg. Med. Chem.* **2003**, *11*, 4049−4057.

(12) Similar calculations with dodecamers of 7-oxo- and 8-oxo-bacteriochlorins possessing 8/7-diethyl groups gave the estimated d_{inner} (6.64/6.62 Å), d_{intra} (9.14/9.34 Å), and d_{HB} (2.07/2.36 Å), and the observed difference was almost the same as in **1**′/**2**′-dodecamers possessing 8/7-dimethyl groups. This result indicated that the principal factor for the different red-shift values 2450/1970 cm^{-1} of self-aggregated **1**/**2** was affected by the situation of the dialkyl group, not by the size of the alkyl substituents.

s, $COOCH_3$), 2.58−2.66 (2H, m, 8-CH_2), 2.62−2.74, 2.22−2.37 (each 2H, m, 17-CH_2CH_2), 1.96/94 (3H, s, 8-CH_3), 1.82/81 (3H, d, J = 8 Hz, 18-CH_3), 0.46−0.51 (3H, m, 8^1-CH_3), −0.65, −1.97 (each 1H, s, NH); ^{13}C NMR ($CDCl_3$) δ 209.4 ($C13^1$), 195.6 (C7), 188.0 ($C3^1$), 173.3, 168.4, 164.13/10, 162.7, 147.6, 147.1, 141.7, 138.3, 136.5, 134.4, 132.5, 128.7, 128.6 (C1, 2, 3, 4, 6, 8, 9, 11, 12, 13, 14, 16, 17^3, 19), 109.0 (C15), 97.8 (C20), 97.6 (C10), 94.40/37 (C5), 54.0 (C8), 52.7 (C17), 51.8 ($C17^5$), 48.9 (C18), 48.2 ($C13^2$), 32.04/31.98 (8-*C*H_2), 30.8 ($C17^2$), 29.8 ($C17^1$), 23.6 ($C18^1$), 23.15/09 (8-*C*H_3), 12.1 ($C12^1$), 11.8 ($C2^1$), 8.91/85 (8^1-*C*H_3); MS (FAB) *m/z* 566.2522 (M^+), calcd for $C_{33}H_{34}N_4O_5$ 566.2529.

Methyl 8-deethyl-7-ethyl-8-oxo-pyropheophorbide-*d* (5): Vis (CH_2Cl_2) λ_{max} 726 (rel intensity, 0.84), 657 (0.15), 601 (0.05), 549 (0.23), 514 (0.11), 479 (0.07), 427 (0.84), 398 nm (1.0); ^{1}H NMR ($CDCl_3$) δ 11.35 (1H, s, 3-CHO), 9.45 (1H, s, 5-H), $9.35_8/35_4$ (1H, s, 10-H), 8.58 (1H, s, 20-H), 5.13, 4.98 (each 1H, d, J = 19 Hz, 13^1-CH_2), 4.38 (1H, m, 18-H), 4.19 (1H, m, 17-H), 3.65 (3H, s, 2-CH_3), 3.65/64 (3H, s, $COOCH_3$), 3.54 (3H, s, 12-CH_3), 2.56−2.64 (2H, m, 7-CH_2), 2.53−2.68, 2.29−2.36, 2.19−2.26 (2H + 1H + 1H, m, 17-CH_2CH_2), 1.90/89 (3H, s, 7-CH_3), 1.77 (3H, d, J = 8 Hz, 18-CH_3), 0.45−0.51 (3H, m, 7^1-CH_3), 0.40, −0.88 (each 1H, s, NH); ^{13}C NMR ($CDCl_3$) δ 209.0 ($C13^1$), 195.1 (C8), 187.9 ($C3^1$), 173.3, 170.9, 168.4, 159.9, 148.6, 145.1, 143.3, 139.1, 137.6, 136.8, 131.2, 129.1, 128.1 (C1, 2, 3, 4, 6, 9, 11, 12, 13, 14, 16, 17^3, 19), 110.1 (C15), 100.5 (C10), 97.0 (C20), 95.6 (C5), 53.4 (C7), 51.8 ($C17^5$), 51.3 (C17), 49.8 (C18), 47.7 ($C13^2$), 31.41/35 (7-*C*H_2), 30.9 ($C17^2$), 29.8 ($C17^1$), 22.9 ($C18^1$), 22.63/58 (7-*C*H_3), 11.8 ($C12^1$), 11.0 ($C2^1$), 8.90 (7^1-*C*H_3); MS (FAB) *m/z* 566.2510 (M^+), calcd for $C_{33}H_{34}N_4O_5$ 566.2529.

Methyl 3-acetyl-7-demethyl-3-devinyl-8-methyl-7-oxo-pyropheophorbide-*a* (10): Vis (CH_2Cl_2) λ_{max} 730 (rel intensity, 1.49), 693 (0.10), 664 (0.09), 550 (0.17), 518 (0.15), 426 (1.00) 395 nm (0.91); ^{1}H NMR ($CDCl_3$) δ 9.81 (1H, s, 5-H), 8.89 (1H, s, 10-H), 8.81 (1H, s, 20-H), 5.28, 5.15 (each 1H, d, J = 19 Hz, 13^1-CH_2), 4.51 (1H, m, 18-H), 4.33 (1H, m, 17-H), 3.65 (3H, s, 12-CH_3), 3.64/63 (3H, s, $COOCH_3$), 3.60 (3H, s, 2-CH_3), 3.32 (3H, s, 3-$COCH_3$), 2.58−2.66 (2H, m, 8-CH_2), 2.59−2.74, 2.23−2.36 (each 2H, m, 17-CH_2CH_2), 1.94/92 (3H, s, 8-CH_3), 1.81/80 (3H, d, J = 8 Hz, 18-CH_3), 0.43−0.51 (3H, m, 8^1-CH_3), −0.62, −2.04 (each 1H, s, NH); MS (FAB) *m/z* 580.2685 (M^+), calcd for $C_{34}H_{36}N_4O_5$ 580.2686.

Methyl 3-acetyl-8-deethyl-7-ethyl-8-oxo-pyropheophorbide-*a* (11): Vis (CH_2Cl_2) λ_{max} 713 (rel intensity, 0.54), 647 (0.14), 594 (0.05), 543 (0.14), 506 (0.11), 474 (0.06), 424 (0.78), 391 nm (1.00); ^{1}H NMR ($CDCl_3$) δ $9.30_9/30_5$ (1H, s, 10-H), 9.03 (1H, s, 5-H), 8.47 (1H, s, 20-H), 5.09, 4.94 (each 1H, d, J = 19 Hz, 13^1-CH_2), 4.34 (1H, m, 18-H), 4.15 (1H, m, 17-H), 3.64_5/63_7 (3H, s, $COOCH_3$), 3.52 (3H, s, 12-CH_3), 3.51 (3H, s, 2-CH_3), 3.19 (3H, s, $COOCH_3$), 2.52−2.59 (2H, m, 7-CH_2), 2.54−2.68, 2.29−2.36, 2.19−2.26 (2H + 1H + 1H, m, 17-CH_2CH_2), 1.86/85 (3H, s, 7-CH_3), 1.75 (3H, d, J = 8 Hz, 18-CH_3), 0.44−0.51 (3H, m, 8^1-CH_3), 0.63, −0.73 (each 1H, s, NH); MS (FAB) *m/z* 580.2691 (M^+), calcd for $C_{34}H_{36}N_4O_5$ 580.2686.

Methyl 7-demethyl-8-methyl-7-oxo-mesopyropheophorbide-*a* (12): Vis (CH_2Cl_2) λ_{max} 713 (rel intensity, 1.16), 677 (0.09), 651 (0.15), 542 (0.16), 509 (0.11), 421 (1.00), 392 nm (0.85); ^{1}H NMR ($CDCl_3$) δ 9.19 (1H, s, 5-H), $8.75_2/75_0$ (1H, s, 10-H), 8.51 (1H, s, 20-H), 5.21, 5.06 (each 1H, d, J = 19 Hz, 13^1-CH_2), 4.38−4.46 (1H, m, 18-H), 4.22−4.27 (1H, m, 17-H), 3.77−3.84 (2H, m, 3-CH_2), $3.63_3/62_7$ (3H, s, $COOCH_3$), 3.59_4/59_3 (3H, s, 12-CH_3), 3.28 (3H, s, 2-CH_3), 2.55−2.62 (2H, m, 8-CH_2), 2.51−2.70, 2.24−2.31 (each 2H, m, 17-CH_2CH_2), 1.92/90 (3H, s, 8-CH_3), $1.78_2/77_6$ (3H, d, J = 8 Hz, 18-CH_3), 1.70 (3H, t, J = 8 Hz, 3^1-CH_3), 0.46−0.53 (3H, m, 8^1-CH_3), −0.10, −1.68 (each 1H, s, NH); MS (FAB) *m/z* 566.2892 (M^+), calcd for $C_{34}H_{38}N_4O_4$ 566.2893.

Methyl 8-deethyl-7-ethyl-8-oxo-mesopyropheophorbide-*a* (13): Vis (CH_2Cl_2) λ_{max} 672 (rel intensity, 0.37), 615 (0.15), 568 (0.06), 527 (0.09), 497 (0.13), 467 (0.07), 423 (0.77), 399 (0.93), 382 nm (1.00); ^{1}H NMR ($CDCl_3$) δ $9.08_4/08_0$ (1H, s, 10-H), 8.09 (1H, s, 5-H), $8.04_5/04_2$ (1H, s, 20-H), 4.95, 4.80 (each 1H, d, J = 19 Hz, 13^1-CH_2), 4.15−4.21 (1H, m, 18-H), 3.98−4.02 (1H, m, 17-H), 3.64/63 (3H, s, $COOCH_3$), 3.56−3.61 (2H, m, 3-CH_2), 3.42 (3H, s, 12-CH_3), 3.11 (3H, s, 2-CH_3), 2.43−2.53 (2H, m, 7-CH_2), 2.41−2.60, 2.18−2.33 (each 2H, m, 17-CH_2CH_2), $1.80_3/79_8$ (3H, s, 7-CH_3), 1.70 (3H, d, J = 8 Hz, 18-CH_3), 1.62 (3H, t, J = 8 Hz, 3^1-CH_3), 0.47−0.53 (3H, m, 7^1-CH_3), 0.08, −2.05 (each 1H, s, NH); MS (FAB) *m/z* 566.2898 (M^+), calcd for $C_{34}H_{38}N_4O_4$ 566.2893.

Zinc Metalation[5a] of Oxo-Bacteriochlorins. To a chloroform solution (20 mL) of oxo-bacteriochlorin **4/5/12/13** (25 μmol), a methanol solution (4 mL) saturated with dihydrated zinc acetate was added and refluxed for 2 days under nitrogen. The reaction mixture was poured into water, washed with 4% aq $NaHCO_3$ and water, dried over Na_2SO_4, and evaporated to dryness. The residue was purified by FCC on silica gel (10−15% diethyl ether/dichloromethane) and recrystallized from chloroform/hexane to give a pure zinc complex (**6/7/14/15** in 85%/83%/84%/85% yields).

Zinc methyl 7-demethyl-8-methyl-7-oxo-pyropheophorbide-*d* (6): Vis (THF) λ_{max} 741 (rel intensity, 3.51), 701 (0.25), 682 (0.24), 595 (0.27), 522 (0.14), 472 (0.64), 452 (0.89), 408 nm (1.00); ^{1}H NMR (1 v/v % pyridine-d_5−$CDCl_3$) δ 11.51 (1H, s, 3-CHO), $9.89_2/89_0$ (1H, s, 5-H), $8.76_8/76_5$ (1H, s, 10-H), 8.70 (1H, s, 20-H), 5.20, 5.08 (each 1H, d, J = 19 Hz, 13^1-CH_2), 4.33 (1H, m, 18-H), 4.25 (1H, m, 17-H), 3.69 (3H, s, 2-CH_3), 3.63 (3H, s, 12-CH_3), $3.59_8/59_4$ (3H, s, $COOCH_3$), 2.58−2.63 (2H, m, 8-CH_2), 2.56−2.64, 2.43−2.50, 2.19−2.27, 2.00−2.11 (each 1H, m, 17-CH_2CH_2), 1.90/87 (3H, s, 8-CH_3), 1.74/72 (3H, d, J = 8 Hz, 18-CH_3), 0.26−0.32 (3H, m, 8^1-CH_3); MS (FAB) *m/z* 628.1672 (M^+), calcd for $C_{33}H_{32}N_4O_5{}^{64}Zn$ 628.1664.

Zinc methyl 8-deethyl-7-ethyl-8-oxo-pyropheophorbide-*d* (7): Vis (THF) λ_{max} 734 (rel intensity, 1.67), 671 (0.22), 588 (0.22), 544 (0.07), 450 (1.00), 408 nm (0.89); ^{1}H NMR (1 v/v % pyridine-d_5−$CDCl_3$) δ 11.25 (1H, s, 3-CHO), 9.32 (1H, s, 10-H), 9.22/21 (1H, s, 5-H), $8.37_4/37_0$ (1H, s, 20-H), 5.02, 4.90 (each 1H, d, J = 19 Hz, 13^1-CH_2), 4.28 (1H, m, 18-H), 4.10 (1H, m, 17-H), 3.58 (6H, s, 2-CH_3 + $COOCH_3$), 3.52 (3H, s, 12-CH_3), 2.48−2.55 (2H, m, 7-CH_2), 2.51−2.56, 2.37−2.43, 2.16−2.23, 2.00−2.08 (each 1H, m, 17-CH_2CH_2), 1.82/80 (3H, s, 7-CH_3), 1.69/68 (3H, d, J = 8 Hz, 18-CH_3), 0.28/23 (3H, t, J = 8 Hz, 7^1-CH_3); MS (FAB) *m/z* 628.1691 (M^+), calcd for $C_{33}H_{32}N_4O_5{}^{64}Zn$ 628.1664.

Zinc methyl 7-demethyl-8-methyl-7-oxo-mesopyropheophorbide-*a* (14): Vis (THF) λ_{max} 723 (rel intensity, 2.20), 685 (0.20), 664 (0.23), 578 (0.21), 538 (0.11), 450 (0.63), 439 (0.75), 396 nm (1.00); ^{1}H NMR (1 v/v % pyridine-d_5−$CDCl_3$) δ 9.04 (1H, s, 5-H), 8.67/66 (1H, s, 10-H), 8.38/37 (1H, s, 20-H), 5.14, 5.01 (each 1H, d, J = 19 Hz, 13^1-CH_2), 4.35 (1H, m, 18-H), 4.17 (1H, m, 17-H), 3.67−3.78 (2H, m, 3-CH_2), 3.59 (3H, s, 12-CH_3), 3.59/57 (3H, s, $COOCH_3$), 3.21 (3H, s, 2-CH_3), 2.52−2.58 (2H, m, 8-CH_2), 2.52−2.58, 2.35−2.42, 2.20−2.27, 1.95−2.01 (each 1H, m, 17-CH_2CH_2), 1.85/84 (3H, s, 8-CH_3), 1.70/69 (3H, d, J = 8 Hz, 18-CH_3), 1.65 (3H, t, J = 8 Hz, 3^1-CH_3), 0.24−0.32 (3H, m, 8^1-CH_3); MS (FAB) *m/z* 628.2024 (M^+), calcd for $C_{34}H_{36}N_4O_4{}^{64}Zn$ 628.2028.

Zinc methyl 8-deethyl-7-ethyl-8-oxo-mesopyropheophorbide-*a* (15): Vis (THF) λ_{max} 678 (rel intensity, 0.89), 625 (0.25), 562 (0.13), 523 (0.14), 443 (1.00), 408 nm (0.85); ^{1}H NMR (1 v/v % pyridine-d_5−$CDCl_3$) δ 9.06 (1H, s, 10-H), $7.87_6/86_8$ (1H, s, 5-H), $7.85_6/85_2$ (1H, s, 20-H), 4.84, 4.72 (each 1H, d, J = 19 Hz, 13^1-CH_2), 4.07 (1H, m, 18-H), 3.90 (1H, m, 17-H), 3.57 (3H, s, $COOCH_3$), 3.45−3.50 (2H, m, 3-CH_2), 3.41 (3H, s, 12-CH_3), 3.03 (3H, s, 2-CH_3), 2.34−2.42 (2H, m, 7-CH_2), 2.29−2.48, 2.01−2.21 (each 2H, m, 17-CH_2CH_2), 1.71/70 (3H, s, 7-CH_3), 1.62 (3H, d, J = 8 Hz, 18-CH_3), 1.56 (3H, t, J = 8 Hz, 3^1-CH_3), 0.31/24 (3H, t, J = 8 Hz, 8^1-CH_3); MS (FAB) *m/z* 628.2021 (M^+), calcd for $C_{34}H_{36}N_4O_4{}^{64}Zn$ 628.2028.

Reduction[5a] of the 3-Formyl to the 3-Hydroxymethyl Group. Zinc 3-formyl-oxo-bacteriochlorin **6** or **7** (20 μmol) was dissolved in 9:1 chloroform/methanol (20 mL), and *t*$BuNH_2$·BH_3 complex (15 mg) was added to the solution, with stirring

at room temperature under nitrogen. When the Q_y maximum of **6/7** at 745/735 nm was completely blue-shifted to the Q_y maximum of the corresponding reduced product **1/2** at 724/683 nm, the reaction mixture was poured into water, washed with aq 0.5% HCl and water, dried over Na_2SO_4, and evaporated to dryness. The residue was purified by FCC on silica gel (1−2% methanol/dichloromethane) and recrystallized from chloroform−methanol/hexane to give pure zinc 3-hydroxymethyl-oxo-bacteriochlorin **1/2** in 92/85% yield.

Zinc methyl 7-demethyl-3-devinyl-3-hydroxymethyl-8-methyl-7-oxo-pyropheophorbide-*a* (1): Vis (THF) λ_{max} 724 (rel intensity, 2.66), 686 (0.22), 666 (0.22), 580 (0.20), 540 (0.08), 441 (0.86), 398 nm (1.00); ^{1}H NMR (1 v/v % pyridine-d_5−$CDCl_3$) δ 9.24 (1H, s, 5-H), 8.72/71 (1H, s, 10-H), $8.48_0/47_5$ (1H, s, 20-H), 5.80 (2H, s, 3-CH_2), 5.16, 5.03 (each 1H, d, J = 19 Hz, 13^1-CH_2), 4.37 (1H, m, 18-H), 4.19 (1H, m, 17-H), 3.60 (3H, s, 12-CH_3), $3.57_4/57_0$ (3H, s, $COOCH_3$), 3.35 (3H, s, 2-CH_3), 2.53−2.59 (2H, m, 8-CH_2), 2.47−2.61, 2.20−2.42 (1H + 3H, m, 17-CH_2CH_2), 1.85/84 (3H, s, 8-CH_3), 1.71/70 (3H, d, J = 8 Hz, 18-CH_3), 0.24−0.31 (3H, m, 8^1-CH_3); MS (FAB) *m/z* 630.1819 (M^+), calcd for $C_{34}H_{34}N_4O_5{}^{64}Zn$ 630.1821.

Zinc methyl 8-deethyl-3-devinyl-7-ethyl-3-hydroxymethyl-8-oxo-pyropheophorbide-*a* (2): Vis (THF) λ_{max} 683 (rel intensity, 0.90), 630 (0.23), 565 (0.12), 525 (0.10), 444 (1.00), 409 nm (0.84); ^{1}H NMR (1 v/v % pyridine-d_5−$CDCl_3$) δ 9.15 (1H, s, 10-H), 8.20/19 (1H, s, 5-H), $8.00_2/7.99_8$ (1H, s, 20-H), 5.61 (2H, s, 3-CH_2), 4.90, 4.77 (each 1H, d, J = 19 Hz, 13^1-CH_2), 4.15 (1H, m, 18-H), 3.96 (1H, m, 17-H), 3.58 (3H, s, $COOCH_3$), 3.45 (3H, s, 12-CH_3), 3.18 (3H, s, 2-CH_3), 2.40−2.48 (2H, m, 7-CH_2), 2.33−2.49, 2.13−2.21, 1.96−2.04 (2H + 1H + 1H, m, 17-CH_2CH_2), 1.74/73 (3H, s, 7-CH_3), 1.65/64 (3H, d, J = 8 Hz, 18-CH_3), 0.30/24 (3H, t, J = 8 Hz, 7^1-CH_3); MS (FAB) *m/z* 630.1829 (M^+), calcd for $C_{34}H_{34}N_4O_5{}^{64}Zn$ 630.1821.

Acknowledgment. Useful discussions with Drs. Tadashi Mizoguchi and Yoshitaka Saga of Ritsumeikan University are gratefully acknowledged. FAB-MS spectra were measured with helpful assistance by Dr. Tomohiro Miyatake of Ryukoku University. This work was partially supported by Grants-in-Aid for Scientific Research (No. 15033271) on Priority Areas (417) from the Ministry of Education, Culture, Sports, Science and Technology (MEXT) of the Japanese Government and for Scientific Research (B) (No. 15350107) from the Japan Society for the Promotion of Science (JSPS). M. K. is grateful for the JSPS Research Fellowship for Young Scientists.

Supporting Information Available: Preparation of 8/7-epimerically pure **1/2**; electronic and CD absorption spectra of 8/7-epimerically pure **1/2** in nonpolar organic solvents and of **1/2** in the solid film; FT-IR spectral change of **1** in a thin film by pyridine vapor and FT-IR spectra of monomeric **1**, **2**, **14**, and **15**; 1D/2D ^{1}H NMR spectra of **1**, **2**, **4**−**7**, **14**, and **15**. This material is available free of charge via the Internet at http://pubs.acs.org.

JO048263P